# FLICKER OF EXTRAGALACTIC RADIO SOURCES AT TWO FREQUENCIES

J. H. SIMONETTI,[1,2] J. M. CORDES,[1,3] AND D. S. HEESCHEN[2]

Flicker of extragalactic sources was investigated by observing 14 flat and 20 steep spectrum sources at 1410 and 2380 MHz from the Arecibo Observatory on 20 successive days. The rms intensity variation of flat spectrum sources is, on average, higher than for steep spectrum sources (2.3% vs. 1.0% at 1410 MHz; 2.8% vs. 1.4% at 2380 MHz). This result confirms earlier work by Heeschen. Through a structure function analysis the variations are shown to have contributions on time scales ranging from at least as small as 1–2 days to greater than 20 days. Variations at the two frequencies show some correlation.

The observed ratio of the flicker amplitude (1410:2380 MHz ≈ 1) is not consistent with a simple interpretation in terms of either "slow refractive" or "fast diffractive" interstellar scintillations. However, data at yet lower frequencies are necessary to rule out completely scintillation explanations of the flicker.

If the variations are intrinsic, they imply brightness temperatures in excess of the inverse Compton limit for an incoherent synchrotron source. Typically, a Lorentz factor for bulk relativistic motion of ∼7 would lower the implied brightness temperature in the rest frame to $10^{12}$ K.

*Subject headings:* radiative transfer — radio sources: galaxies — radio sources: variable

## I. INTRODUCTION

Extragalactic radio sources are known to vary on a wide range of time scales and with different properties in different wavelength ranges. Variability at centimetric wavelengths with time scales $\gtrsim 1$ yr is generally consistent with outbursts in canonical electron synchrotron sources in active galactic nuclei (AGNs). Low-frequency variable (LFV) sources show month-to-year fluctuations at subgigahertz frequencies that imply brightness temperatures (when using time scales to infer angular size) much larger than the $\sim 10^{12}$ K limit associated with inverse Compton scattering in incoherent synchrotron sources (e.g., Kellermann and Pauliny-Toth 1969, 1981). In this paper we consider the "flicker" phenomenon discovered recently by Heeschen (1982, 1984) which appears as $\sim 2\%$ variations of flat-spectrum sources on time scales of days at 9 cm wavelength.

The relationship of the flicker to the other forms of variability is uncertain and it is the aim of this paper to present results which may distinguish intrinsic from extrinsic effects. Intrinsic flicker would share the excess brightness temperatures inferred from LFV sources. However, it has been recently proposed (Rickett, Coles, and Bourgois 1984) that both low-frequency variability and flicker may be associated with refraction from electron-density irregularities in the Galaxy. This proposal arises from an extrapolation of slow (months to years) and fast (minutes to hours) intensity variations of pulsars associated with refraction and diffraction in the interstellar medium. It is obviously important to diagnose whether extrinsic effects can account for most variability which, interpreted as an intrinsic phenomenon, implies excessive brightness temperatures and generally large energy input injection rates from the AGN.

In this paper we analyze dual-frequency observations of flat and steep-spectrum sources made at Arecibo Observatory over a 20 day period (1983 September 1–20). The aim was to confirm the reality of the phenomenon first identified by Hees-

chen using the 300′ telescope at Green Bank, to further explore the time structure of the flicker, and to determine the frequency dependence of the flicker. Our results confirm the original results and demonstrate that variations occur on daylike time scales, rather than being due to ramp functions selected out from much longer scale variations by the short observing span. The lack of any strong frequency dependence suggests that the flicker is probably intrinsic, although propagation effects cannot be absolutely ruled out.

In § II we describe the observing and reduction procedure which yields the basic amplitude variations (or modulation indices) discussed in § III. The structure function results follow in § IV, while the necessary definitions and error analysis for the structure functions are presented in the Appendix. The case against interstellar scintillation (ISS) is examined in § V where the applicable scintillation theory is reviewed. In § VI relativistic source motion is treated as a solution to the brightness-temperature problems which arise if the variations are assumed intrinsic to the sources. The conclusions are presented in § VII.

## II. OBSERVING AND REDUCTION PROCEDURE

### a) Source List

Approximately equal numbers of flat and steep radio spectrum sources were chosen from the catalog of Kühr et al. (1979, 1981) in preprint form. Sources were selected if they were within the declination range of the Arecibo telescope, and if their relative positions enabled us to observe the greatest number within the daily 8 hr observing period. If the spectral index $\alpha$ (where $S_\nu \propto \nu^{-\alpha}$) was less than 0.4 (as determined from the Kühr et al. 1979 spectrum), the source was labeled a flat-spectrum source. We attempted to choose unambiguously flat or steep spectrum objects (Table 1).

### b) Observing Procedure

Signals from dual circularly polarized feeds and 1410 MHz cooled FET receivers and 2380 MHz maser receivers were used. The half-power beamwidths of the Arecibo telescope are 3′.3 and 2′.0, the system temperatures are 40 and 45 K, and the

[1] Department of Astronomy, Cornell University, and the National Astronomy and Ionosphere Center.
[2] The National Radio Astronomy Observatory.
[3] Alfred P. Sloan Foundation Fellow.

sensitivities are 8.0 and 6.5 K Jy$^{-1}$, for the 1410 and 2380 MHz systems. At both frequencies observations were made with a 20 MHz bandwidth, 10 ms smoothing time constant, and a sampling rate of 0.01 s.

All observations were made at night, in order to minimize any changes in the telescope structure due to uneven heating, found to be a large source of error in daytime observations at Green Bank (Heeschen 1984).

We recorded one triplet drift scan per frequency per polarization for each source on each day of the 20 day period. The triplet consisted of a drift scan at the source declination, and at positive and negative declination offsets of $\pm 50''$ and $\pm 30''$ at 1410 and 2380 MHz, respectively. The drift scans had durations of 120 s at 1410 MHz, and 70 s at 2380 MHz. A 1 K noise tube was fired for 5 s at the beginning of each drift scan.

### c) Data Reduction and Editing

Each source observation (triplet drift scan) yielded a source-to-cal ratio proportional to the flux density, and derived through a two-step process: (1) Source-to-cal ratios (peak source response/noise tube) were determined for each scan of a triplet and (2) were combined into a nominal source-to-cal ratio corrected for possible pointing errors. The two polarizations were processed separately. After obviously bad triplets (e.g., due to inference) were edited out, the rms variation and structure functions were calculated for each source at each frequency and polarization.

Values for the source and noise tube deflections within a drift scan were obtained by fitting a linear baseline to selected portions of the scan, averaging over the noise tube signal, and fitting a parabola to the peak region of the source response. The maximum of a parabolic fit to the individual scan ratios was taken to be the nominal source-to-cal ratio for the triplet,

while the location of the maximum with respect to the central scan declination yielded the declination pointing error. The resultant source-to-cal ratio and declination pointing error are accurate to at least 1% and less than 10%, respectively, for a point source which lies within the north and south declination offsets. Examination of the drift scans indicated that all sources are much smaller in extent than 2.'0.

For each source, time series of the source-to-cal ratio and the declination pointing error versus day, as well as the original scans themselves, were examined for evidence of interference or systematic errors. All sources with rms source-to-cal variations in excess of 2%–3% were studied more carefully for "bad" days. Nearly all large and fast changes (>5% over 1 day) could be tracked down to interference. One source (0446 + 11) was observed with an incorrect telescope position (off by 26'' in declination as indicated by comparison of the positions in Kühr et al. 1979, 1981), resulting in large, 2380 MHz flux variations anticorrelated with day-by-day pointing errors, rendering the data useless. A second source (2309 + 18) showed similar behavior at 2380 MHz, and although a Kühr et al. (1981) position is not available as confirmation, it is probable that our observing coordinates were incorrect. The 2380 MHz data for this second source were also ignored. One polarization showed consistently higher source-to-cal variations, and rather than combine the two polarizations, only the results for the polarization with lower variations were considered here and in further analysis.

Figure 1 shows the final source-to-cal and declination pointing error measurements at both frequencies for the BL Lac source, 0235 + 16. The error bars for the source-to-cal values are estimates based on the structure function analysis described in § IV and are 1.1% for 1410 MHz and 1.6% for 2380 MHz.
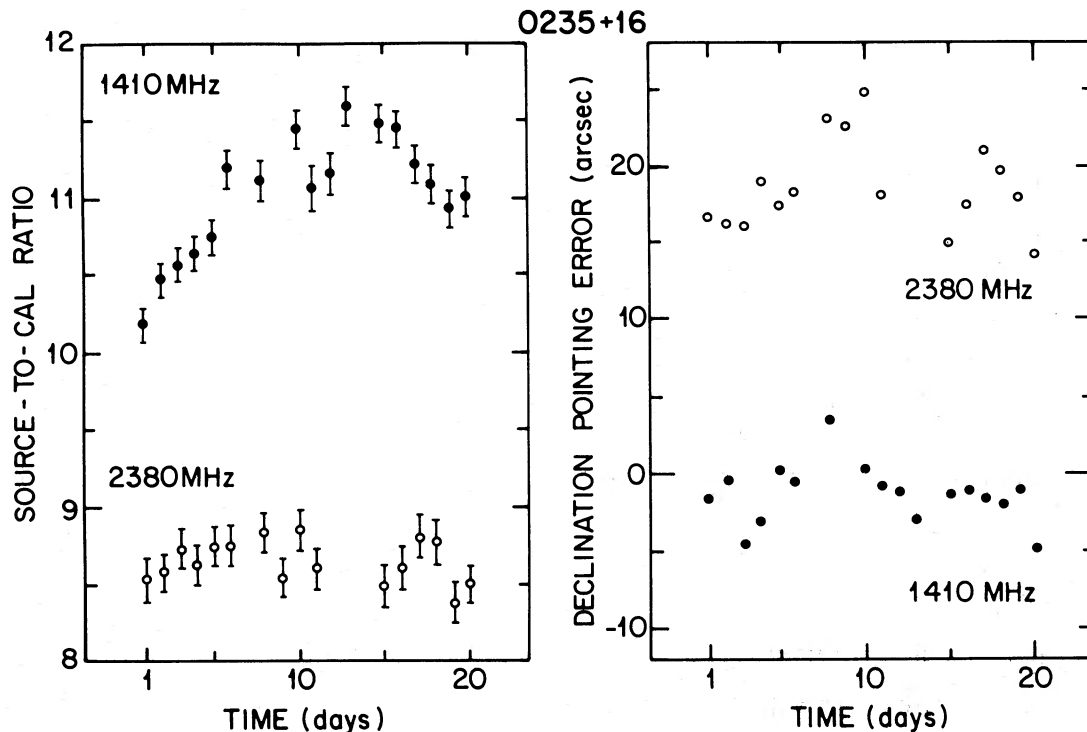


FIG. 1.—Source-to-cal ratio and declination pointing error time series for 0235 + 16

Mean fluxes were computed using 0017+15 as a flux calibrator with 1410 and 2380 MHz fluxes determined from Kühr et al. (1979). Table 1 contains the final values of $\mu$ = rms/mean source-to-cal and the flux densities, and spectral indices derived using our data. Two sources (2230+11, 2251+13) were classified as steep spectrum based on Kühr et al. (1979) spectra, while our observed spectral indices for these sources are less than 0.4. Both sources have been left in the "S" (steep-spectrum) class; relabeling them as "F" (flat-spectrum) sources does not significantly affect our class-average results, while, as discussed below, they may more appropriately belong to the "S" class on the basis of our flicker study.

### III. VARIABILITY OF FLAT SPECTRUM AND STEEP SPECTRUM SOURCES

The values of $\mu$ presented in Table 1 are used to construct the histograms shown in Figure 2 for the flat- and steep-spectrum sources separately. Figure 3 most dramatically shows the difference in behavior between the sources with small-to-

negative spectral indices and the large spectral index sources. A division between sources that vary over the 20 day period and sources that do not lies at $\alpha \approx 0.1$–0.2, comparable to our break between the F and S classes. Steep-spectrum sources generally have small values of $\mu$ ($\lesssim 0.025$), whereas flat-spectrum sources have a much broader range of values, extending to 0.07. Some "F" sources have small values of $\mu$ at both frequencies; others have large values at both frequencies, while others have one large and one small value at either frequency (Table 2).

Correlations were searched for, but not found, between $\mu$ and galactic latitude, galactic longitude, mean declination pointing error, the telescope azimuth and zenith angle, and the corresponding standard deviations of those angles. The absence of a correlation between $\mu$ and galactic latitude may imply that ISS does not play a role in the variations, but the thickness of the galactic scattering material is not well known (Cordes, Weisberg, and Boriakoff 1985), so this is a weak argument. At both frequencies, a scatter plot of $\mu$ versus flux density

TABLE 1

INDIVIDUAL SOURCE RESULTS

| | | | | | | | 1410 MHz | | | 2380 MHz | | |
|---|---|---|---|---|---|---|---|---|---|---|---|---|
| SOURCE | R.A.(1950.0) | Decl.(1950.0) | $l^{II}$ | $b^{II}$ | $C^a$ | $\alpha$ | $\mu$ (%) | $S_v^b$ (Jy) | Slope$^c$ | $\mu$ (%) | $S_v^b$ (Jy) | Slope$^c$ |
| 0007+17......... | 00$^h$07$^m$59$^s$8 | 17°07'38" | 109°2 | −44°4 | F | −0.12 | 1.8 | 0.86 | 0.02(0.15) | 1.0 | 0.91 | 0.05(0.29) |
| 0119+11......... | 01 19 03.1 | 11 34 10 | 134.6 | −50.4 | F | −0.03 | 1.8 | 1.07 | 0.64(0.16) | 2.1 | 1.09 | 0.59(0.10) |
| 0119+24......... | 01 19 54.2 | 24 46 52 | 131.8 | −37.3 | F | 0.19 | 1.7 | 0.70 | −0.07(0.17) | 1.5 | 0.63 | −0.06(0.16) |
| 0147+18......... | 01 47 05.5 | 18 42 26 | 141.6 | −41.8 | F | −0.08 | 2.9 | 0.38 | 0.29(0.09) | 2.3 | 0.40 | −0.15(0.15) |
| 0235+16......... | 02 35 52.6 | 16 24 05 | 156.8 | −39.1 | F | −0.02 | 3.5 | 2.80 | 0.82(0.08) | .1.6 | 2.83 | 0.05(0.17) |
| 0306+10......... | 03 06 21.0 | 10 17 53 | 169.2 | −39.7 | F | −0.41 | 3.0 | 0.55 | 1.05(0.10) | 1.5 | 0.68 | 0.14(0.14) |
| 0317+18......... | 03 17 00.3 | 18 50 38 | 164.9 | −31.5 | F | −1.22 | 2.4 | 0.37 | 0.88(0.11) | 4.4 | 0.70 | 1.29(0.07) |
| 0446+11$^d$....... | 04 46 20.5 | 11 16 45 | 187.4 | −20.7 | F | −0.5$^e$ | 1.4 | 0.63 | 0.56(0.21) | ... | ... | ... |
| 0454+06......... | 04 54 25.6 | 06 40 29 | 192.7 | −21.7 | F | −0.09 | 1.3 | 0.52 | 0.01(0.25) | 3.5 | 0.55 | 1.04(0.13) |
| 2144+09......... | 21 44 42.5 | 09 15 51 | 65.8 | −32.3 | F | 0.04 | 4.9 | 0.83 | 1.83(0.10) | 7.1 | 0.81 | 1.04(0.13) |
| 2236+12......... | 22 36 06.4 | 12 27 10 | 79.7 | −38.8 | F | −0.18 | 3.3 | 0.24 | 0.85(0.17) | 5.4 | 0.27 | 0.40(0.12) |
| 2251+15......... | 22 51 29.5 | 15 52 54 | 86.1 | −38.2 | F | −0.31 | 0.8 | 13.26 | 0.09(0.15) | 2.5 | 15.57 | 1.14(0.15) |
| 2328+10......... | 23 28 08.6 | 10 43 46 | 93.1 | −47.1 | F | −0.28 | 1.8 | 1.12 | 0.45(0.15) | 1.8 | 1.30 | 0.22(0.15) |
| 2344+09......... | 23 44 03.8 | 09 14 06 | 97.5 | −50.1 | F | −0.05 | 1.0 | 1.94 | 0.20(0.14) | 2.3 | 1.98 | 0.13(0.13) |
| 0017+15......... | 00 17 49.8 | 15 24 16 | 112.0 | −46.5 | S | 1.10 | 1.0 | 2.22 | 0.07(0.18) | 1.0 | 1.25 | 0.03(0.29) |
| 0030+19......... | 00 30 01.3 | 19 37 23 | 116.9 | −42.8 | S | 0.60 | 0.9 | 2.08 | −0.15(0.27) | 0.9 | 1.52 | 0.03(0.31) |
| 0035+12......... | 00 35 39.2 | 12 11 10 | 117.9 | −50.3 | S | 0.41 | 1.5 | 1.10 | 0.03(0.15) | 2.2 | 0.89 | −0.09(0.18) |
| 0042+13......... | 00 42 46.3 | 13 24 03 | 120.7 | −49.2 | S | 0.65 | 0.9 | 1.43 | 0.05(0.17) | 1.9 | 1.02 | 0.50(0.14) |
| 0124+18......... | 01 24 12.3 | 18 57 46 | 134.4 | −42.9 | S | 0.52 | 0.7 | 1.43 | 0.02(0.22) | 1.1 | 1.09 | 0.18(0.25) |
| 0138+13......... | 01 38 28.7 | 13 38 23 | 140.9 | −47.2 | S | 0.69 | 0.9 | 2.80 | −0.14(0.20) | 1.3 | 1.95 | 0.07(0.16) |
| 0312+10......... | 03 12 38.6 | 10 01 41 | 170.9 | −38.9 | S | 0.64 | 0.8 | 1.67 | 0.04(0.13) | 2.0 | 1.20 | 0.09(0.14) |
| 0316+16......... | 03 16 09.1 | 16 17 40 | 166.6 | −33.6 | S | 0.52 | 1.0 | 7.92 | −0.06(0.16) | 1.2 | 6.04 | 0.33(0.26) |
| 0333+12......... | 03 33 40.5 | 12 52 40 | 173.2 | −33.3 | S | 0.73 | 1.3 | 2.19 | −0.10(0.20) | 1.3 | 1.49 | 0.23(0.21) |
| 0422+08......... | 04 22 54.9 | 08 26 18 | 186.2 | −27.1 | S | 0.95 | 1.2 | 1.25 | −0.07(0.20) | 1.8 | 0.76 | 0.26(0.16) |
| 0459+25......... | 04 59 54.3 | 25 12 12 | 177.7 | −9.9 | S | 0.67 | 1.1 | 5.71 | −0.01(0.29) | 1.3 | 4.03 | −0.06(0.17) |
| 0518+16......... | 05 18 16.5 | 16 35 27 | 187.4 | −11.3 | S | 0.36 | 0.7 | 8.16 | 0.09(0.18) | 1.4 | 6.75 | 0.15(0.16) |
| 2138+14......... | 21 38 23.2 | 14 24 23 | 69.1 | −27.7 | S | 0.72 | 0.9 | 1.43 | −0.34(0.71) | 0.9 | 0.98 | 0.98(1.74) |
| 2209+08......... | 22 09 32.4 | 08 04 25 | 69.8 | −37.6 | S | 0.60 | 0.8 | 1.82 | 0.07(0.34) | 1.2 | 1.33 | 0.01(0.26) |
| 2230+11......... | 22 30 07.8 | 11 28 23 | 77.4 | −38.6 | S | 0.23 | 0.9 | 6.53 | −0.13(0.07) | 1.1 | 5.80 | 0.56(0.50) |
| 2247+13......... | 22 47 16.1 | 13 15 13 | 83.1 | −39.8 | S | 0.50 | 1.7 | 1.48 | 0.02(0.15) | 2.0 | 1.13 | 0.23(0.17) |
| 2247+14......... | 22 47 56.9 | 14 03 56 | 83.9 | −39.2 | S | 0.36 | 1.1 | 2.15 | −0.12(0.22) | 1.0 | 1.78 | 0.05(0.25) |
| 2251+13......... | 22 51 51.7 | 13 25 48 | 84.4 | −40.3 | S | 0.47 | 1.2 | 1.51 | 0.21(0.24) | 1.6 | 1.18 | 0.10(0.17) |
| 2252+12......... | 22 52 35.9 | 12 57 28 | 84.3 | −40.8 | S | 0.73 | 0.9 | 2.73 | 0.11(0.20) | 1.8 | 1.86 | −0.05(0.15) |
| 2309+18......... | 23 09 36.5 | 18 29 09 | 92.5 | −38.2 | S | 1.0$^e$ | 1.1 | 1.32 | 0.03(0.19) | ... | ... | ... |

$^a$ Spectral class: F (flat) or S (steep) spectrum.
$^b$ High zenith angle telescope gain corrections were made using curves supplied by Haynes and Giovanelli 1984 and S. Ostro (private communication).
$^c$ The slopes are of the log-log first-order structure function with 1 $\sigma$ error in parentheses.
$^d$ The right ascension and declination of 0446+11 are 04$^h$46$^m$21$^s$20 and 11°16'18".9 in Kühr et al. 1981.
$^e$ Spectral index estimated from spectrum in Kühr et al. 1979.
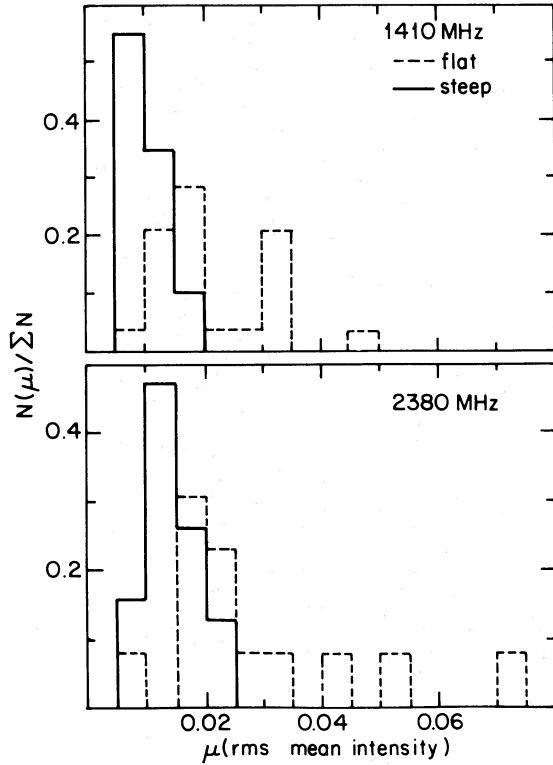
FIG. 2.—Histograms of $\mu$ (= rms/mean intensity) for flat- and steep-spectrum sources.

shows large $\mu$ sources have lower flux densities than other sources, but this is a selection effect since the steep-spectrum sources have higher flux densities than most of those with flat spectra at our observation frequencies.

### IV. TIME SCALES OF VARIABILITY FROM STRUCTURE FUNCTION ANALYSIS

In this section we present a structure function analysis of the daily measurements which provides information on the tempo-

TABLE 2
OBSERVED VARIATION AMPLITUDES

| Spectral Class | Frequency (MHz) | $\langle\mu(\%)\rangle$ | $\sigma_\mu$ |
|---|---|---|---|
| F(flat)............. | 1410 | 2.26 | 1.13 |
| | 2380 | 2.84 | 1.76 |
| S(steep) ........... | 1410 | 1.02 | 0.27 |
| | 2380 | 1.43 | 0.42 |

ral structure of the intensity variations. Structure functions are defined in the Appendix and are similar to auto- and cross-correlation functions. For example, the first-order cross structure function between two time sequences $x_1(t)$ and $x_2(t)$ is

$$D_{12}^{(1)}(\tau) = \langle [x_1(t + \tau) - x_1(t)][x_2(t + \tau) - x_2(t)] \rangle , \qquad (1)$$

and removes any DC components in the time series. Structure functions of order $M$ remove polynomials of order $M - 1$ from the time series; the result depends only upon any stationary random process in the series and remaining higher order trends. This feature of higher order structure functions makes them ideal probes of a short-correlation time scale random process ("flicker") superposed on long-correlation time scale trends (such as month-to-year flux variations). The analysis demonstrates the presence of variations in the F sources on time scales as small as 1 or 2 days which are not evident in the S sources. Such short time scale variations are clearly present in averages of structure functions over the class of F sources, and in the results for some individual sources.

We computed first- and second-order structure functions of the quantity $f$ = source-to-cal/$\langle$source-to-cal$\rangle$ for each source at both frequencies (where angular brackets denote an average over the entire 20 day observing period). Normalization with respect to the 20 day average prevented any one source from dominating the structure functions when averaged over all sources. A first-order cross-frequency structure function was also computed for each source in order to investigate any correlation between the time sequences for the two frequencies. Finally, grand-average first- and second-order structure functions were calculated for the two classes of sources.
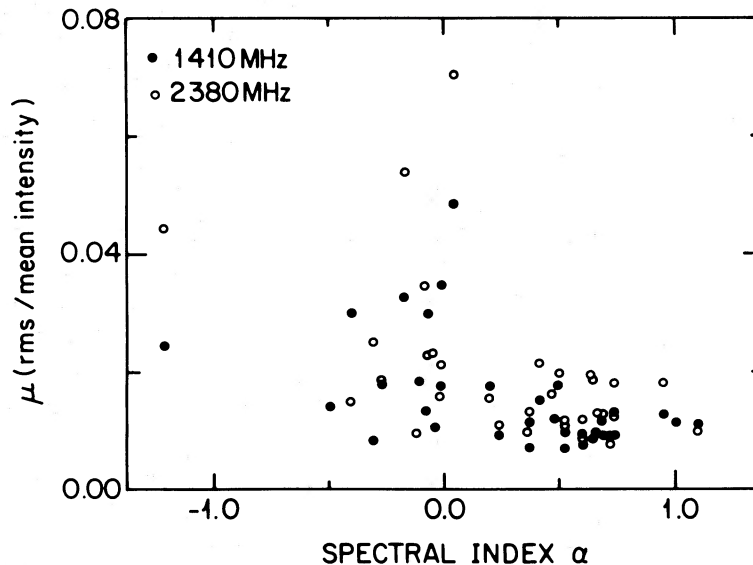


FIG. 3.—Observed $\mu$ vs. spectral index $\alpha$
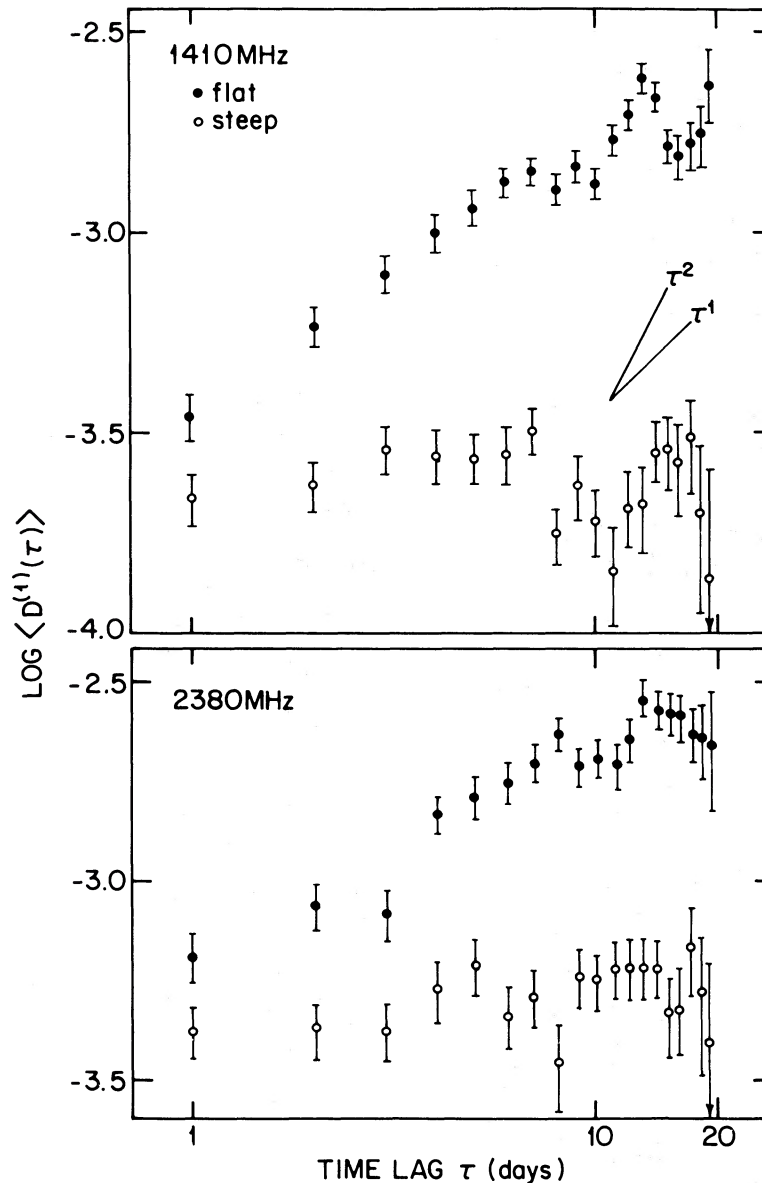
Fig. 4.—First-order grand-average structure functions. A 45° line has unity slope. Error bars are $\pm 1\,\sigma$.

As discussed in the Appendix, there is a contribution to the structure functions from the random error, $\delta f$, inherent in the process. Therefore, we examined the "raw" structure functions and "corrected" structure functions where a constant contribution due to measurement error was subtracted (measurement error estimated from the first-order grand-average structure functions for S sources as $\sigma_{\delta f} = 0.011$ and 0.016 for 1410 and 2380 MHz, respectively; see below). We have plotted one example of a set of "raw" and "corrected" structure functions in Figure 8. All other structure functions plotted (or represented by fitted slopes in Table 1) are "raw." We have analyzed uncorrected structure functions because (1) we have no firm basis for estimating the corrections accurately and (2), although the applied correction does increase the logarithmic slope of the structure functions, it does not alter, for a reasonable upper limit to the measurement error contribution, the conclusion that daylike structure exists in the source variations (see below).

## a) The Grand-Average Results for the Flat- and Steep-Spectrum Sources

That daylike variations are present in the time series for F sources is evident from consideration of both the first-order and second-order grand-average structure functions (Fig. 4 and 5).

The first-order grand-average structure functions $\langle D^{(1)}(\tau)\rangle$ for the F sources have logarithmic slopes less than 2 over the entire range of lags, even if we attempt to correct them for the contribution due to measurement error. Using an upper limit to the measurement error contribution at 1410 MHz of $\langle D^{(1)}(\tau = 1 \text{ day})\rangle$, implying $\sigma_{\delta f} = 0.013$, yields a corrected structure function of logarithmic slope 1.24 for $2 \le \tau \le 6$ days, decreasing to less than unity at larger $\tau$. A slope of 2 would have been consistent with (but does not necessarily imply) the presence of variations only on time scales greater than the observing period. Therefore, the results indicate that variations
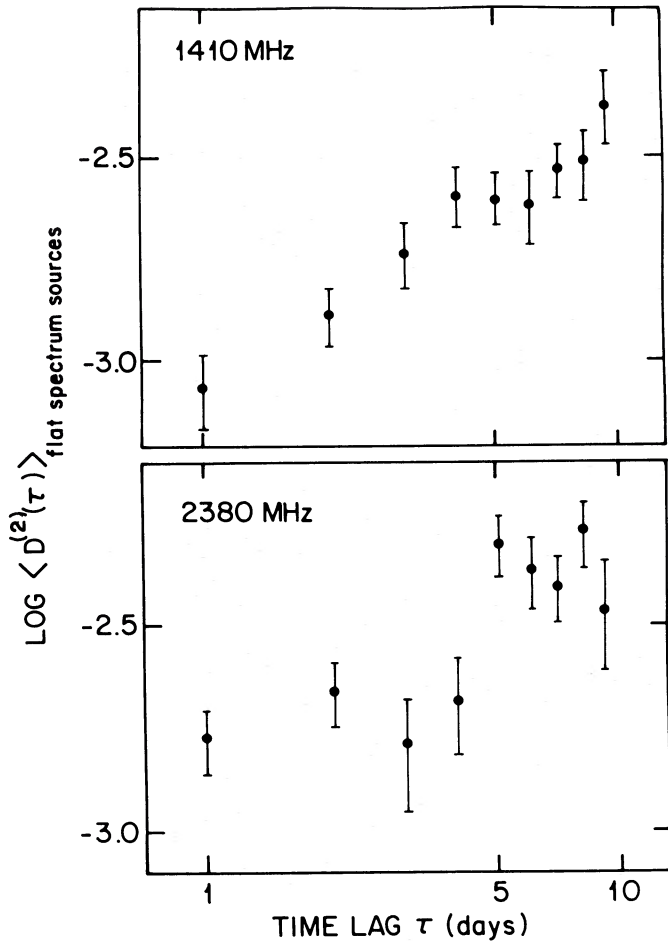
FIG. 5.—Second-order grand-average structure functions for flat-spectrum sources.

occur on time scales as small as 1 to 2 days and at least as large as 19 days. Structure smaller than 1 day may also be present, since we cannot find a definite lower limit to the region with slope less than 2. The structure functions of the S sources have approximately zero slopes that are consistent with white noise time series that are probably dominated by measurement errors.

The second-order structure functions remove any linear trends in the time series and therefore *directly* demonstrate the presence of daylike structure for the F sources. The second-order F source structure functions imply essentially the same flicker amplitude as from the first-order structure functions. Moreover, the second-order structure functions have slopes less than 4, even after correction for the measurement error contribution, indicating that quadratic flux variations do not dominate the structure functions. Variability over the 20 day span must be caused by daylike structure because a simple linear function (which would approximate a 20 day segment of a long-term variation) would have yielded a zero slope and small-amplitude second-order structure function. The grand-average results for S sources still show a zero slope.

### b) Flicker of Individual Flat-Spectrum Sources

As can be seen from Figures 2, 3, 6, and 7, the flat-spectrum sources display a range of behavior: some flicker, some do not. Those flat-spectrum sources with high signal-to-noise structure functions confirm, on an individual source basis, the conclusions drawn above from the grand-average results.

#### i) 0235+16

This source, a BL Lac object which also shows centimetric and low-frequency variability, has well-determined first and second-order structure functions at 1410 MHz, but zero-slope structure functions at 2380 MHz (Fig. 1 and 8). The logarithmic slopes of the 1410 MHz structure functions (given in Table 1), even after correction for the measurement error contribution, are well below the values expected for a source with contributing time scales only larger than 20 days (note that the corrected structure functions in Fig. 8 are shifted down, for plotting, by 0.5 on the log scale). At the same time the 2380
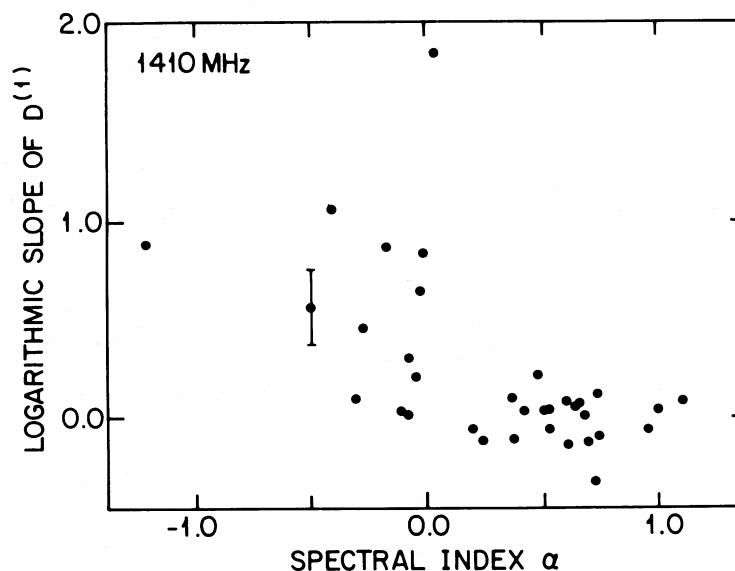


FIG. 6.—Logarithmic slope of the first-order structure function at 1410 MHz vs. spectral index. A typical ±1 σ error bar is shown.
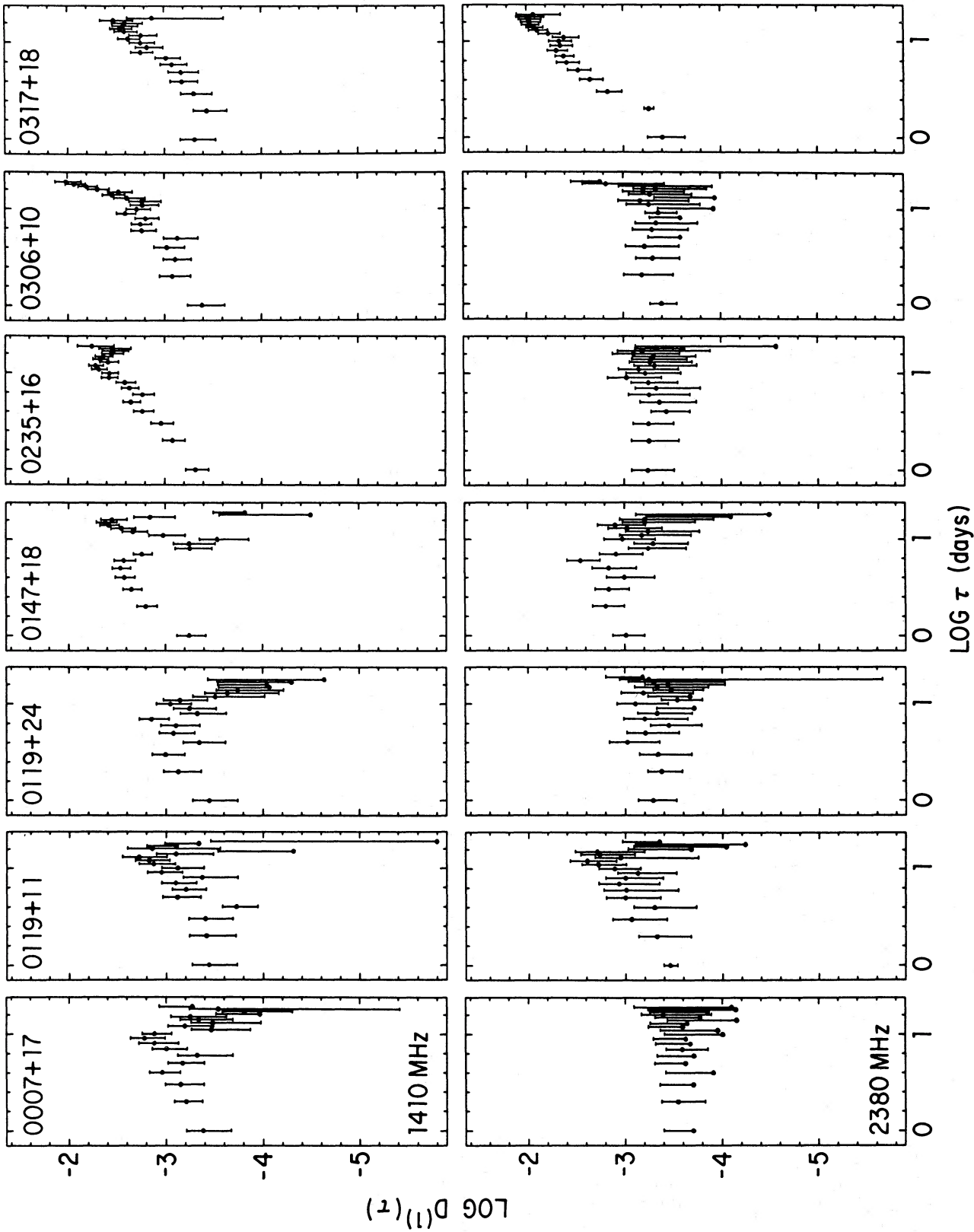
FIG. 7.—First-order structure functions at 1410 and 2380 MHz for the flat-spectrum (F) sources listed in Table 1. Error bars are ±1 σ. Where the uncertainty for a given point is greater than the point's value, only the upper portion of the error bar is drawn.

52

FIG. 7—Continued

LOG τ (days)

LOG D(1)(τ)

2344+09 2328+10 2251+15 2236+12 2144+09 0454+06 0446+11

2380 MHz 1410 MHz

53
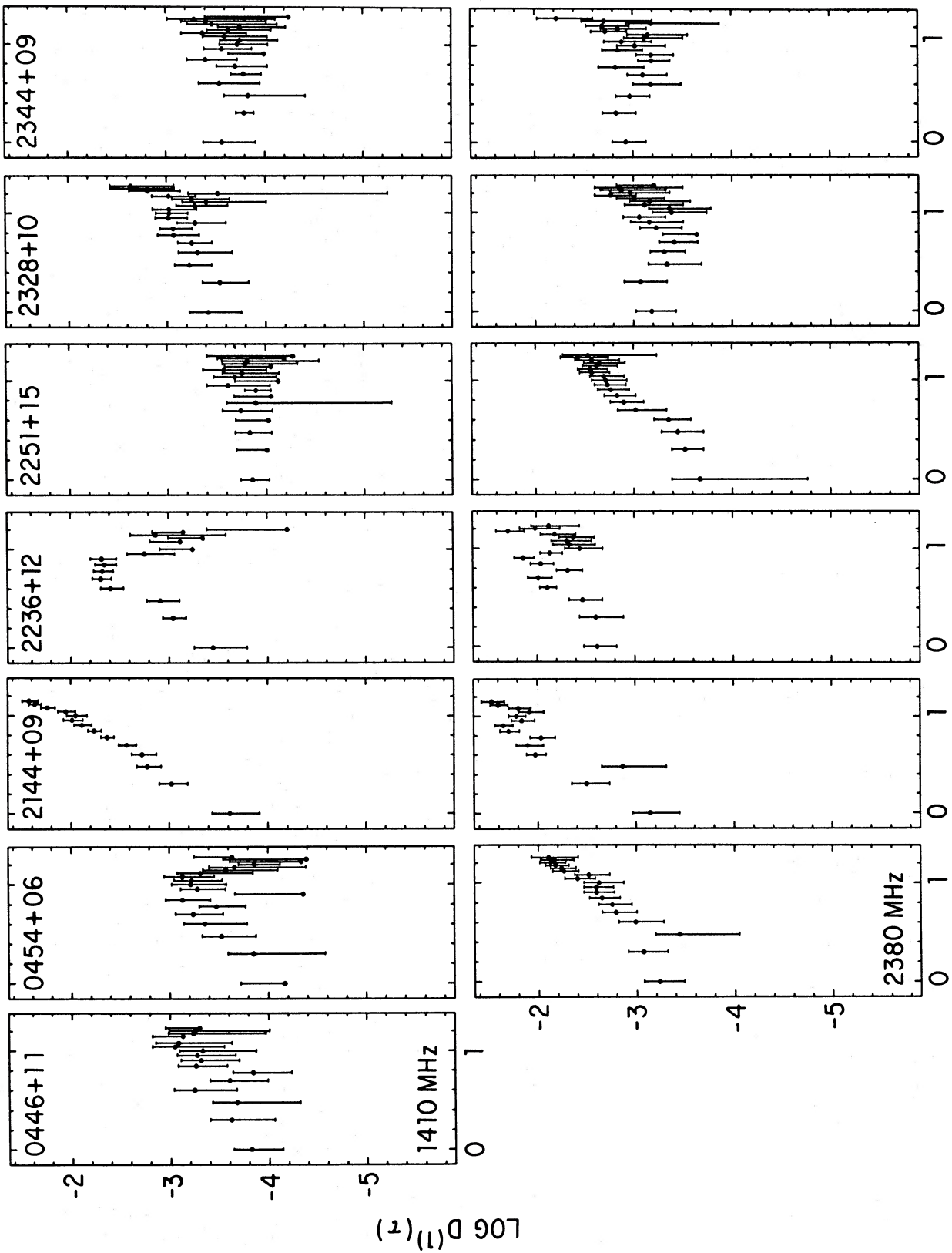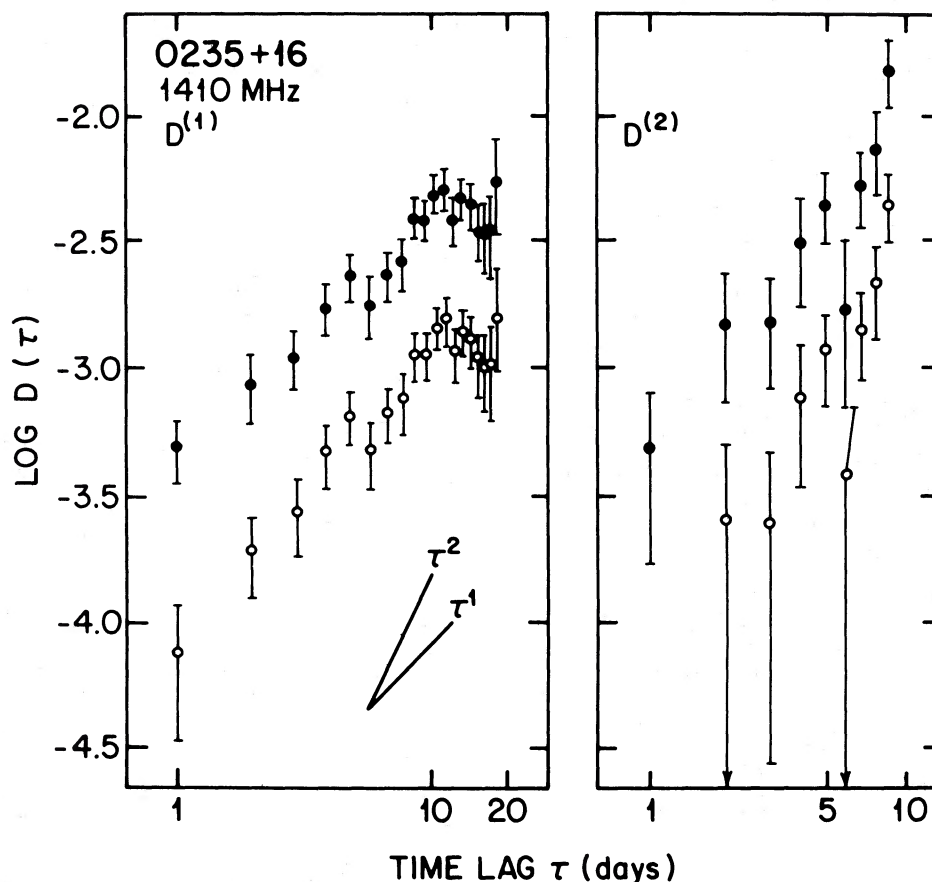
FIG. 8.—First- and second-order structure functions at 1410 MHz for 0235 + 16 (*filled data points*). Open data points display the results of subtracting $2\sigma^2_{\delta f}$ and $6\sigma^2_{\delta f}$ from the first- and second-order structure functions, respectively, discussed in the text as the structure functions corrected for measurement error contributions. Note that the "corrected" structure functions have been shifted down by 0.5 on the log scale to reduce confusion in the plot.

MHz results are similar to those for any steep-spectrum source (no structure).

### ii) 0306 + 10

This is another example of an F source with structure at 1410 MHz but not at 2380 MHz. The fitted slopes imply small time scale variations.

### iii) 0317 + 18

This particular flat spectrum source has well-determined structure functions at both frequencies (Fig. 9). Short time scales (at least as small as 1 day) are evident.

### iv) 0454 + 06

Here we have a source with only a 2380 MHz first-order structure function that is well out of the measurement noise. Its logarithmic slope before, and after correction, is not well below 2 as for the other above sources, but it still suggests short time scale variations.

### v) 2144 + 09

This source has a first-order structure function logarithmic slope at 1410 MHz that is equal to 2 before and certainly after correction for measurement error. Its second-order structure function slope at 1410 MHz is consistent with zero. These results imply a purely linear flux variation throughout our 20 day period, in agreement with an examination of the source-to-cal time sequence. Therefore, the variations in the flux of 2144 + 09 are dominated by time scales probably greater than

our observing period at 1410 MHz. At 2380 MHz, however, the structure functions have slopes indicative of shorter time scale contributions.

### vi) 2251 + 15 (3C 454.3)

Another object with well-studied centimetric and low-frequency variability is 2251 + 15. In our data, it shows structure only at 2380 MHz, with short variability time scales.

### c) The Cross-Frequency Structure Function

In Figure 10 we present the first-order grand-average cross-frequency structure function normalized by the autofrequency results, which can be interpreted as a correlation coefficient between the two frequencies. Measurement noise should be uncorrelated. It is clear from the figure that there is correlation between the variations (long-term plus flicker) in the F sources at 1410 and 2380 MHz, as evidenced by values systematically nonzero and occasionally greater than 0.5. Values at specific lags are not indicative of correlation on a comparable time scale since all time scales contribute to the structure function at any given lag $\tau$; therefore, the occurrence of larger values at $10 < \tau < 15$ days cannot be attributed to correlation over such time scales only. There is also some marginal correlation present for the S sources as well, which may be real but is probably an indication of a small correlation between the measurement error for the two frequencies (perhaps due to correlated pointing errors).
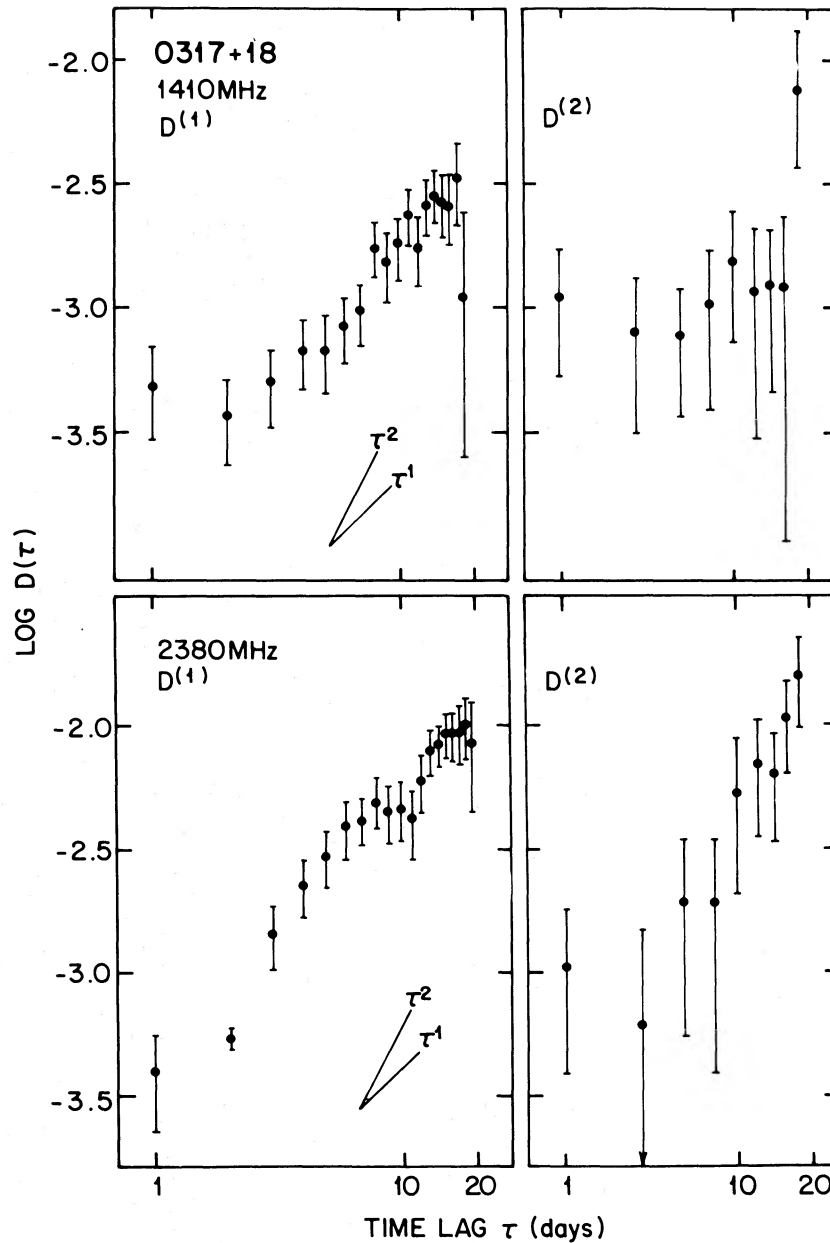
FIG. 9.—Structure functions for 0317 + 18

Since source variations are larger than measurement errors for flat-spectrum sources (as reflected in the autofrequency structure functions [Figs. 4 and 5]), values of $\langle D_{12}^{(1)}/[\langle D_{11}^{(1)}\rangle\langle D_{22}^{(1)}\rangle]^{1/2} \gtrsim 0.5$ are indicative of a cross-frequency structure function dominated by correlated source variations. Furthermore, *short* time scales contribute substantially to the source variations as implied by the second-order autofrequency structure functions. Therefore, short time scale flicker appears to be correlated over a large frequency range, although the dominance of daylike time scales in the correlated variations is not completely established at this point.

### V. INTERSTELLAR SCINTILLATION

In the previous two sections we established that flat-spectrum sources show variability on time scales of 1–20 days, which seems to be absent in steep-spectrum sources.

One obvious candidate source of variability is some form of scintillation. Heeschen (1984) has reviewed the salient features of ionospheric, interplanetary, interstellar, and circumsource scintillation, most of which seem implausible when compared with the implied time scales of the variability.

Given the recent proposal made by Rickett, Coles, and Bourgois (1984) that refractive fluctuations from electron density irregularities in the ISM may cause intensity variations of extragalactic radio sources, we compare the observational results of the flicker with predictions for such "slow" refractive variations as well as predictions for "fast" diffraction induced variations. After a brief description of the ISS theory as it applies to our problem, we discuss the case against explanations of the flicker as either slow or fast scintillation.

#### a) ISS Theory

A plane wave passing through a thin screen containing a medium of randomly irregular refractive index produces a dif-
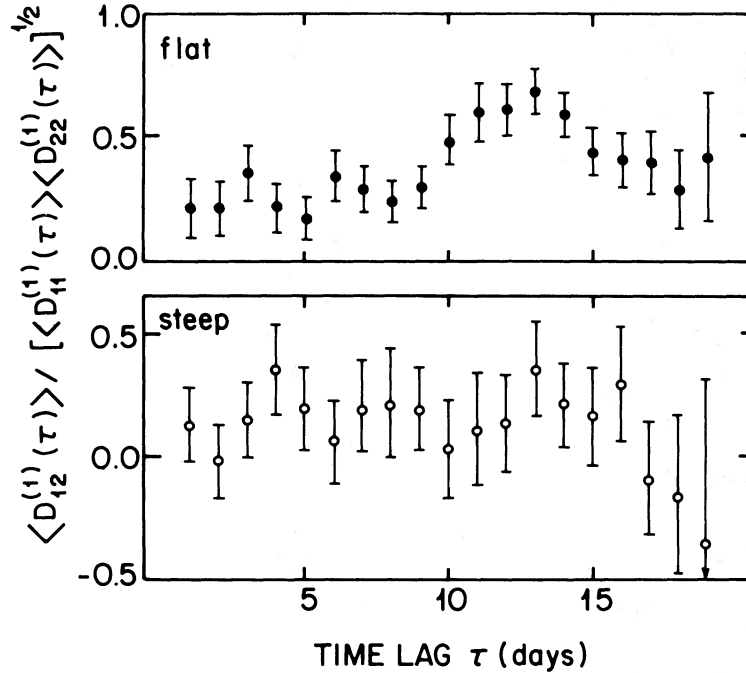
FIG. 10.—First-order grand-average cross-frequency structure function normalized by the autostructure function values. Upper and lower panels display the results for flat- and steep-spectrum sources, respectively.

fraction pattern at a distance $L$ from the screen with spatial scales

$$s_1 = \eta^{-1}s_F \,, \qquad (2)$$
$$s_2 = \eta s_F \,,$$

where $s_1$ and $s_2$ are "refractive" and "diffractive" scales (e.g., Prokhorov et al. 1975), $s_F = (\lambda L)^{1/2}$ is the Fresnel scale, and $\eta \approx (\Delta v/4\pi v)^{1/2}$, while $\Delta v$ is the decorrelation bandwidth of the fast ISS. In the strong scattering limit $\eta \ll 1$, while in the weak scattering limit $\eta$ saturates at unity and the two spatial scales are the same.

The recent work of Cordes, Weisberg, and Borikoff (1985), based on a consideration of the scintillations of 76 pulsars, indicates we may safely assume our observations at 1410 and 2380 MHz are within the strong scattering regime at $\lambda \gtrsim 6$ cm. As they show, besides a clumped turbulent medium of low filling factor, low scale height, and relatively high $C_n^2$, there exists a turbulent medium with filling factor $f > 0.5$, scale height at least as large as $H = 500$ pc, and $C_n^2 \approx 10^{-3.5}$ m$^{-20/3}$ at the midpoint of the galactic plane (where turbulent density variations are described by a power-law power spectrum $P_{\delta n_e} = C_n^2[\text{wavenumber}]^{-\alpha}$; $\alpha = 11/3$ for a Kolmogorov spectrum). A reasonable lower limit for $C_n^2$, allowing for any variations, is $10^{-4}$ m$^{-20/3}$. We emphasize that the scale height of the turbulent medium appears to be larger than the scale height $H_{\text{disp}} \approx 380$ pc of those electrons that dominate pulsar dispersion measures. The large-scale height turbulent medium would be responsible for any scintillation of extragalactic sources with galactic latitude $\gtrsim 10°$. From Rickett, Coles, and Bourgois (1984), we find

$$v_{\text{sat}} = 4700\left(\frac{C_n^2}{10^{-4}\,\text{m}^{-20/3}}\right)^{0.35}\left(\frac{H}{500\,\text{pc}}\right)^{0.65}(\sin|b|)^{-0.65}\,\text{MHz}$$

$$(3)$$

for the frequency at which scintillations would just saturate for extragalactic sources and a Kolmogorov spectrum. The value $C_n^2 = 10^{-3.5}$ yields $v_{\text{sat}} = 7000$ MHz at the galactic pole for $H = 500$ pc. Since our largest latitude source is at $b^{\text{II}} = 50°$, scintillations should be strong at 1410 and 2380 MHz.

In the strong scattering limit with relative motion transverse to the line-of-sight of velocity $V$, the two time scales for variability of the intensity are

$$t_{\text{slow}} \approx s_1/V \propto \lambda^{2.2} \,,$$
$$t_{\text{fast}} \approx s_2/V \propto \lambda^{-1.2} \,, \qquad (4)$$

for the slow and fast ISS. The wavelength dependences apply for a medium with a Kolmogorov spectrum of electron density irregularities. Such a spectrum is inferred from observations of pulsar fast ISS for length scales in the range $10^{10}$–$10^{11}$ cm, and there is some evidence that an extrapolation of the same power-law spectrum to larger scales (at least $10^{15}$ cm) is consistent with the data on slow fading of pulsars (i.e., slow scintillation) (Rickett, Coles, and Bourgois 1984). This extrapolation of the irregularity spectrum is controversial, however, since the opposite conclusion has been reached by Hewish (1980).

In the strong scattering limit, and for small observing bandwidth (less than $\Delta v$), point sources scintillate (fast ISS) with unity modulation. A source of large angular size $\theta_{\text{source}}$ will have quenched fast ISS, and if large enough, quenched slow ISS. The critical sizes for this low-pass filtering to be substantial are

$$\theta_{c_1} = s_1/L \,,$$
$$\theta_{c_2} = s_2/L \,. \qquad (5)$$

Since $\theta_{c_1} \gg \theta_{c_2}$ in the strong scattering limit, a source showing fast ISS will also show slow ISS on a longer time scale, although the converse is not true.

If we assume the source size is independent of wavelength, and $\theta_{\rm source} \gg \theta_{c_1}$, then the modulation indices in the strong scattering limit are

$$M_1 \approx (\theta_{c_1}/\theta_{\rm source})M_{1,\rm pt} ,$$
$$M_2 \approx (\theta_{c_2}/\theta_{\rm source})M_{2,\rm pt} , \tag{6}$$

where $M_{1,\rm pt}$ and $M_{2,\rm pt}$ are the modulation indices for a point source. In strong scattering $M_{2,\rm pt} = 1$ independent of the form of the electron-density irregularity spectrum, whereas $M_{1,\rm pt}$ depends strongly on the form of the spectrum of electron-density irregularities (Prokhorov et al. 1975; Goodman and Narayan 1985). In the following we assume that $M_{1,\rm pt} = 1$ and is wavelength independent.

### b) Slow ISS

If the flicker is slow ISS for $\theta_{\rm source} \approx 50\theta_{c_1}$ and $\theta_{\rm source}$ is independent of $\lambda$, we expect $\mu(1410 \text{ MHz})/\mu(2380 \text{ MHz}) = 3.2$. For the flat-spectrum sources the ratio $\mu(1410)/\mu(2380)$ has a mean and rms deviation of 1.02 and 0.64. Even if we consider only the most strongly varying F sources, the result is very nearly the same. Although the flicker appears broad-band (Fig. 10), as would be consistent with either slow ISS or intrinsic causes, slow ISS seems ruled out on the basis of the observed flicker amplitudes.

One possibility to explore is that the source size at our observing frequencies may be dominated by scattering in an extragalactic medium (or galactic halo). If $\theta_{\rm source} \propto \lambda^2$, the expected ratio for slow ISS is $\mu(1410)/\mu(2380) = 1.1$, consistent with the flicker results. Such circumstances ($\mu \propto \lambda^{0.2}$) may allow slow ISS to explain flicker, but then it would be inconsistent with LFV. Stated differently, slow ISS cannot explain both LFV and flicker as we understand them at present. It would be premature to adopt the broadening slow-ISS scenario for flicker over a slow-ISS explanation for LFV, since the flicker case requires the additional assumption of $\lambda^2$ scattering in some hitherto unknown medium.

### c) Fast ISS

The predicted ratio for fast ISS when the source size is independent of $\lambda$ is $\mu(1410)/\mu(2380) = 0.5$, and is not ruled out by the observed ratio. However, the apparent correlation between flicker variations at 1410 and 2380 MHz is not consistent with fast ISS as extrapolated from pulsar studies.

Furthermore, if the extrapolation of the Kolmogorov spectrum to large scales is valid, there are two more arguments against fast ISS being a cause of flicker.

First, if we assume that LFV is caused by slow ISS with $\mu(400 \text{ MHz}) \approx 0.1$, then slow ISS at 1410 MHz would have $\mu \approx 0.006$ (if source size is independent of $\lambda$) and any fast ISS at 1410 MHz would necessarily have a much smaller amplitude [since $M(\rm fast) \ll M(\rm slow)$].

Second, in the opposite extreme where we assume that the observed 1410 MHz flicker is due to fast ISS, then slow ISS would also occur as a 100% modulation on time scales larger than 20 days (for any wavelength dependence of source size). No such modulations have ever been reported at 1410 MHz.

We conclude that fast ISS is probably not the cause of flicker.

### VI. INTRINSIC VARIABILITY

In this section we assume the flicker of flat-spectrum sources is intrinsic, and show this implies brightness temperatures greater than the inverse Compton limit, and excessive X-ray fluxes. Relativistic bulk motion of the emitting regions removes these problems. We calculate the necessary Doppler factor $\delta = [\Gamma(1 - \beta \cos \theta)]^{-1}$, where $\Gamma = (1 - \beta^2)^{-1/2}$ is the Lorentz factor, for source motion at angle $\theta$ from the source-observer line.

Following the analysis of Marscher et al. (1979), if we assume no bulk relativistic source motion, the ratio of the brightness temperature calculated from variability measurements to the Compton-limited temperature is

$$\frac{T_v}{10^{12} \text{ K}} \approx 1400 \left(\frac{S_m}{\text{Jy}}\right)\left(\frac{v_m}{\text{GHz}}\right)^{-2}\left(\frac{D}{\text{Gpc}}\right)^2$$
$$\times \left(\frac{\Delta S_v}{0.01 S_v}\right)^2 \left(\frac{\Delta t_v}{\text{day}}\right)^{-2} (1 + z)^{-0.8} , \tag{7}$$

where $S_m$ is the flux density at cutoff frequency $v_m$, $D$ and $z$ are the distance and redshift of the source, $\Delta S_v/0.01 S_v$ is the observed percentage variation in the flux density, and $\Delta t_v = [(d \ln S_v/dt)(S_v/\Delta S_v)]^{-1}$ is a variation time scale. For a relativistically moving source the above ratio (eq. [7]) is equal to $\delta^{3.2}$, with a ratio of 1400 corresponding to $\delta \approx 9.6$, or a Lorentz factor of $\Gamma \approx 6.8$ for $\theta \approx 0$, comparable to the relativistic factors derived for superluminal motions seen with VLBI (Kellermann and Pauliny-Toth 1981). Since a large fraction of our F sources flicker, solving the associated brightness temperature problem through relativistic bulk motion would perhaps require an isotropic outflow, as opposed to motion along jets of small opening angle.

It should also be mentioned that a coherent radiation mechanism could account for the implied high brightness temperatures. As pointed out by Rees, Begelman, and Blandford (1981), coherent emission cannot be ruled out considering conditions within the source core (e.g., $B \approx 10^4$ G). If this is the answer, then the sizes derived on the basis of the observed variability time scales would imply that fast diffractive ISS should have been seen, contrary to observation (e.g., Dennison and Condon 1981). However, the loophole here is that the sources, as observed, may be broadened in an extragalactic medium or galactic halo, leading to quenched diffractive ISS.

Utilizing equation (7) of Marscher et al. (1979), for the X-ray flux expected from a source, we find, roughly, for $\alpha = 0.25$ (a typical spectral index for compact AGN sources)

$$F_x(2\text{–}10 \text{ keV}) \approx \left(\frac{S_m}{\text{Jy}}\right)^{4.5}\left(\frac{D}{\text{Gpc}}\right)^7\left(\frac{\Delta S_v}{0.01 S_v}\right)^7$$
$$\times \left(\frac{\Delta t_v}{\text{day}}\right)^{-7} (1 + z)^{-6.5} \text{ ergs s}^{-1} \text{ cm}^{-2} \tag{8}$$

as the integrated flux in the 2–10 keV range for $\delta = 1$. The sensitivity quoted by Marscher et al. is $\approx 2 \times 10^{-11}$ ergs s$^{-1}$ cm$^{-2}$. If any set of variable sources contains some flickering objects, then the experiment of Marscher et al. and other searches would have easily detected these X-ray flux levels, while no such X-ray flux has been detected from variable ratio sources. Since $F_x \propto \delta^{-2(3\alpha + 5)}$, the value $\delta \approx 9.6$ would lower the predicted flux to less than the sensitivity limit of the observations.

### VII. CONCLUSIONS

Our analysis of dual-frequency observations of flat- and steep-spectrum extragalactic radio sources suggests the following conclusions:

1. As first reported by Heeschen (1982, 1984), flat-spectrum sources have, over a 20 day period, larger intensity variations (rms $\approx$ 2%), in general, than steep-spectrum sources.

2. A structure function analysis demonstrates a qualitative difference in the time series of flat- and steep-spectrum sources. Steep-spectrum sources have time series entirely consistent with uncorrelated measurement errors. In contrast, distinct structure, with a range of daylike time scales, is present in the time series of flat-spectrum sources. We refer to the variations with daylike time scales as "flicker." Flicker may even occur on time scales less than 1 day.

3. Flicker is apparently broad-band, contributing to correlated intensity variations at 1410 and 2380 MHz. However, more work is needed to firmly establish a large correlation bandwidth for flicker.

4. With essentially no wavelength dependence, flicker appears to be a distinctly different phenomenon than low-frequency variability (LFV), which has a decreasing amplitude with decreasing wavelength. Observations at lower frequencies would be useful to see if the wavelength independence of the flicker amplitude holds deep in the strong scattering regime.

5. Flicker and LFV cannot both be caused by slow (refractive) interstellar scintillations (ISS). Flicker is consistent with slow ISS of a source broadened (size $\propto \lambda^2$) through scattering in an extragalactic medium, but such a process would not produce the observed characteristics of LFV. Slow ISS of a source with size independent of wavelength may account for LFV but cannot be the cause of flicker.

6. In light of the apparent correlation between flicker at 1410 and 2380 MHz, it seems that fast (diffractive) ISS is not the cause of the short time scale variations. A firmly established broad-band nature for flicker would definitely rule out fast ISS as a cause of flicker.

7. Since propagation effects may not cause flicker, intrinsic variability at the $\sim 2$% level and on daylike time scales must be considered. The excessive brightness temperatures implied by the variations can be reduced below the self-Compton limit if we assume the presence of relativistic bulk motions with Lorentz factors comparable to those inferred for sources showing superluminal component separation velocities.

## APPENDIX

### STRUCTURE FUNCTIONS AND ERROR ANALYSIS

We define here the structure functions used in § IV, and derive the associated uncertainties in structure functions estimated from a finite time sequence of data.

The $M$th-order structure function for the function $\phi(t)$ is defined as (following Rutman 1978)

$$D_\phi^{(M)}(t, \tau) = \langle [\Delta_\phi^{(M)}(t, \tau)]^2 \rangle , \tag{A1}$$

where the angular brackets denote an ensemble average, and

$$\Delta_\phi^{(M)}(t, \tau) = \sum_{n=0}^{\infty} (-1)^n \binom{M}{n} \phi(t + [M - n]\tau) \tag{A2}$$

is the $M$th increment of $\phi(t)$. Structure functions are useful in analyzing functions of the form

$$\phi(t) = \sum_{k=0}^{N} \frac{A_k}{k!} t^k + x_s(t) , \tag{A3}$$

where $x_s(t)$ is a stationary process and the $A_k$ are random variables. The structure function of order $M > N$ is determined by the process $x_s(t)$ alone, since the $M$th order increment of an $N$th order polynomial is zero. For $M \leq N$, only the polynomial terms of order greater than or equal to $M$ contribute to the increment. A simple linear function has a first-order structure function proportional to $\tau^2$, while its second-order structure function is zero. Correlated stationary noise has the first- and second-order structure functions

$$D_\phi^{(1)}(\tau) = 2\sigma_\phi^2[1 - \rho_\phi(\tau)] , \tag{A4}$$

$$D_\phi^{(2)}(\tau) = 6\sigma_\phi^2[1 + \tfrac{1}{3}\rho_\phi(2\tau) - \tfrac{4}{3}\rho_\phi(\tau)] , \tag{A5}$$

where $\rho_\phi(\tau)$, with $\rho_\phi(0) \equiv 1$, is the autocorrelation function and $\sigma_\phi^2$ is the variance of the process.

A most useful feature of structure functions as far as we are concerned is their ability to discern the range of time scales that contribute to the variations in a data set. In the limit of $\tau \gg T_1$, where $T_1$ is the largest correlation time scale of the process,

$$D_\phi^{(M)}(\tau) = \sum_{n=0}^{\infty} \binom{M}{n} \sigma_\phi^2 = \begin{cases} 2\sigma_\phi^2 , & M = 1 ; \\ 6\sigma_\phi^2 , & M = 2 . \end{cases} \tag{A6}$$

In the limit of $\tau \ll T_0$, where $T_0$ is the smallest correlation time scale present in the sequence,

$$D_\phi^{(M)}(\tau) \propto \tau^{2M} , \tag{A7}$$

while for $T_0 \ll \tau \ll T_1$ the dependence on $\tau$ will be a power less than or equal to $2M$ (the exact dependence determined by the power spectrum of the process).

For a finite sequence of measurements $f(i)$, $i = 1, 2, \ldots, N$, the first- and second-order structure functions are estimated by

$$D_f^{(1)}(k) = \frac{1}{N^{(1)}(k)} \sum_{i=1}^{N} w(i)w(i+k)[f(i+k) - f(i)]^2 , \tag{A8}$$

$$D_f^{(2)}(k) = \frac{1}{N^{(2)}(k)} \sum_{i=1}^{N} w(i)w(i+k)w(i+2k)[f(i+2k) - 2f(i+k) + f(i)]^2 , \tag{A9}$$

where

$$N^{(1)}(k) = \sum w(i)w(i+k) , \qquad N^{(2)}(k) = \sum w(i)w(i+k)w(i+2k) , \tag{A10}$$

and the weighting factor $w(i)$ is 1 if a measurement exists for the $i$th interval, 0 otherwise.

Equations (A8) and (A9) are used to obtain our individual-source first- and second-order structure functions at 1410 and 2380 MHz separately. The first-order cross-frequency structure function for each source is estimated by

$$D_{12}^{(1)}(k) = \frac{1}{N_{12}^{(1)}(k)} \sum_{i=1}^{N} w_1(i)w_1(i+k)w_2(i)w_2(i+k)[f_1(i+k) - f_1(i)][f_2(i+k) - f_2(i)] , \tag{A11}$$

with $N_{12}^{(1)}(k)$ defined in analogy with $N^{(1)}(k)$ and $N^{(2)}(k)$. The time sequences for 1410 and 2380 MHz are $f_1$ and $f_2$, respectively. Finally, the grand-average structure functions for the flat- and steep-spectrum sources are averages over the structure functions of the sources in each class weighted by $N^{(M)}(k)$, or

$$\langle D^{(M)}(k) \rangle \equiv \sum_s N^{(M)}(k; s)D^{(M)}(k; s) \bigg/ \sum_s N^{(M)}(k; s) , \tag{A12}$$

where $s$ labels the sources in a particular class.

Let $f(i) = F(i) + \delta f(i)$, where $F(i)$ is the value we would measure if our measurements had zero uncertainty and $\delta f(i)$ is the measurement error. Assuming the random measurement errors are described by white noise (or, equivalently, a process having a correlation time scale $\ll 1$ day), the structure functions are

$$D_f^{(M)}(k) = D_F^{(M)}(k) + \begin{cases} 2\sigma_{\delta f}^2 , & M = 1 ; \\ 6\sigma_{\delta f}^2 , & M = 2 ; \\ 0 , & \text{cross-frequency} ; \end{cases} \tag{A13}$$

where $\sigma_{\delta f}^2$ is the measurement noise variance. The squared uncertainties in the estimated structure functions are roughly (assuming a complete time series of $N$ samples)

$$\sigma^2(k; M = 1) \approx \frac{8\sigma_{\delta f}^2}{N^{(1)}(k)} D_f^{(1)}(k) , \tag{A14}$$

$$\sigma^2(k; M = 2) \approx \frac{24\sigma_{\delta f}^2}{N^{(2)}(k)} D_f^{(2)}(k) , \tag{A15}$$

$$\sigma^2(k; \text{cross}) \approx \frac{2}{N_{12}^{(1)}(k)} [\sigma_{\delta f_2}^2 D_{f_1}^{(1)}(k) + \sigma_{\delta f_1}^2 D_{f_2}^{(1)}(k)] . \tag{A16}$$

The uncertainties for the grand-average structure functions follow straightforwardly from equations (A14)–(A16) and equation (A12).

## REFERENCES

Cordes, J. M., Weisberg, J. M., and Boriakoff, V. 1985, *Ap. J.*, in press.
Dennison, B., and Condon, J. J. 1981, *Ap. J.*, **246**, 91.
Goodman, J., and Narayan, R. 1985, preprint.
Haynes, M. P., and Giovanelli, R. 1984, *A.J.*, **89**, 758.
Heeschen, D. S. 1982, in *IAU Symposium 97, Extragalactic Radio Sources*, ed. D. S. Heeschen and C. M. Wade (Dordrecht: Reidel), p. 327.
———. 1984, *A.J.*, **89**, 1111.
Hewish, A. 1980, *M.N.R.A.S.*, **192**, 799.
Kellermann, K. I., and Pauliny-Toth, I. I. K. 1969, *Ap. J. (Letters)*, **155**, L71.
———. 1981, *Ann. Rev. Astr. Ap.*, **19**, 373.
Kühr, H., Nauber, U., Pauliny-Toth, I. I. K., and Witzel, A. 1979, Max-Planck-Institut für Radioastronomie preprint, No. 55.
Kühr, H., Witzel, A., Pauliny-Toth, I. I. K., and Nauber, U. 1981, *Astr. Ap. Suppl.*, **45**, 367.
Marscher, A. P., Marshall, F. E., Mushotzky, R. F., Dent, W. A., Balonek, T. J., and Hartman, M. F. 1979, *Ap. J.*, **233**, 498.
Prokhorov, A. M., Bunkin, F. V., Gochelashvily, K. S., and Shishov, V. I. 1975, *Proc. IEEE*, **63**, 790.
Rees, M. J., Begelman, M. C., and Blandford, R. D. 1981, *Ann. NY Acad. Sci.*, **375**, 254.
Rickett, B. J., Coles, W. A., and Bourgois, G. 1984, *Astr. Ap.*, **134**, 390.
Rutman, J. 1978, *Proc. IEEE*, **66**, 1048.

JAMES M. CORDES: Space Sciences Building, Cornell University, Ithaca, NY 14853

D. S. HEESCHEN and JOHN H. SIMONETTI: National Radio Astronomy Observatory, Edgemont Road, Charlottesville, VA 22903